BIOCHEMISTRY
including biophysical chemistry & molecular biology

ACCELERATED PUBLICATION

pubs.acs.org/biochemistry

Caspase-6 Latent State Stability Relies on Helical Propensity

Sravanti Vaidya and Jeanne A. Hardy*

Department of Chemistry, 710 North Pleasant Street, University of Massachusetts, Amherst, Massachusetts 01003, United States

Supporting Information

ABSTRACT: Caspase-6 is an apoptotic protease that also plays important roles in neurodegenerative disorders, including Huntington's and Alzheimer's diseases. Caspase-6 is the only caspase known to form a latent state in which two extended helices block access to the active site. These helices must convert to strands for binding substrate. We probed the interconverting region and found that the absence of helix-breaking residues is more critical than a helix-bridging, hydrogen-bond network for formation of the extended conformation. In addition, our results suggest that caspase-6 must undergo a transition through a low-stability intermediate to bind the active-site ligand. Mature caspase-6 is capable of adopting a latent state not observed in any other caspase. The absence of any helix-breaking residues allows caspase-6 to adopt the extended helical conformation. When we introduced helix-breaking residues similar to those seen in caspase-3 or -7, the structure and stability of the latent state were compromised.

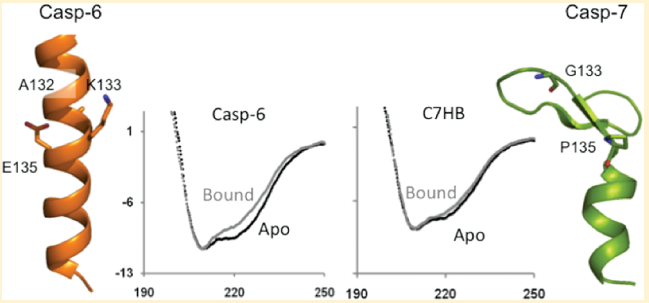

Caspases make up a class of cysteine-aspartate proteases that play important roles in apoptosis, inflammation, and development. Caspase-6 was originally classified primarily as an apoptotic executioner protease, as cleavage of the procaspase-6 zymogen by upstream caspases appeared to be essential for activation. During programmed cell death, caspase-6, along with caspase-3 and -7, cleaves critical factors, including nuclear and cytoskeletal proteins, leading to the demise of the cell. It has become clear recently that caspase-6 also performs several non-apoptotic roles, including axonal pruning during development[1] and B cell activation and differentiation.[2] Currently, caspase-6 is most widely recognized for its role in cleaving neuronal substrates involved in neurodegeneration.[3] It has become clear that caspase-6 plays important roles in Huntington's,[4] Alzheimer's,[5] and Parkinson's diseases,[6] where cleavage of substrates by caspase-6 is a causative event in the development of each of these pathologies. As a result, despite historical difficulties in developing caspase-directed drugs, caspase-6 is now viewed as a promising drug target for neurodegeneration. The structure and regulation of caspase-6 are clearly unique among caspases, so a better understanding of caspase-6 structure and function is essential for developing caspase-6 specific therapies, which may prove to be important in the treatment of several neurodegenerative diseases.

The structures of caspase-6 in the immature zymogen form,[7] in the mature unliganded (apo) form,[8,9] and with the active site bound by a peptide inhibitor[7] have recently been determined. The active site-bound and zymogen forms of caspase-6 are similar to all other caspases, but in apo mature caspase-6, the 60's region (amino acids 57−70) and the 130's region (amino acids 128−142) are in extended helices that have not been observed previously (Figure 1A). The formation of these helices causes the outward rotation of the 90's helix and movement of the L1 loop. In the apo state, the loop above the 130's helix occupies the substrate binding groove and the catalytic dyad is mispositioned for catalysis, suggesting that the apoenzyme is in a latent state.[8] Thus, to bind substrate, caspase-6 must undergo a dramatic reorganization of the 60's, 90's, and 130's helices and the L1 loop. Currently, perhaps the most compelling questions about caspase-6 are why and how it forms the extended helical state and what biological roles of caspase-6 require this unique conformation.

RESULTS AND DISCUSSION

Inspection of the caspase-6 apo structure reveals a helix-bridging hydrogen-bond network between the 130's and 60's helices that can form in caspase-6 but not in other caspases because of both sequence and conformation. The interactions in this network position caspase-6 in the latent (catalytically inactive) conformation. In apo caspase-6, the side chain of the catalytic base, His121, which is located in the loop at the top of 130's helix, is held 9 Å from the catalytic nucleophile Cys163, preventing catalysis. His121 is held in this inactive position by Tyr128, Glu63 (60's helix), and Glu53 (the L1 loop above the 60's helix). Glu63 and Glu53 make salt bridges with the side chain of His121. Tyr128 (130's helix) makes a salt bridge with the backbone amide of His121 (Figure 1B). Position 53 is a glutamate residue only in caspase-1 and -6, and position 63 is a

Received: February 2, 2011
Revised: March 6, 2011
Published: March 07, 2011

dx.doi.org/10.1021/bi2001664 | *Biochemistry* 2011, 50, 3282–3287

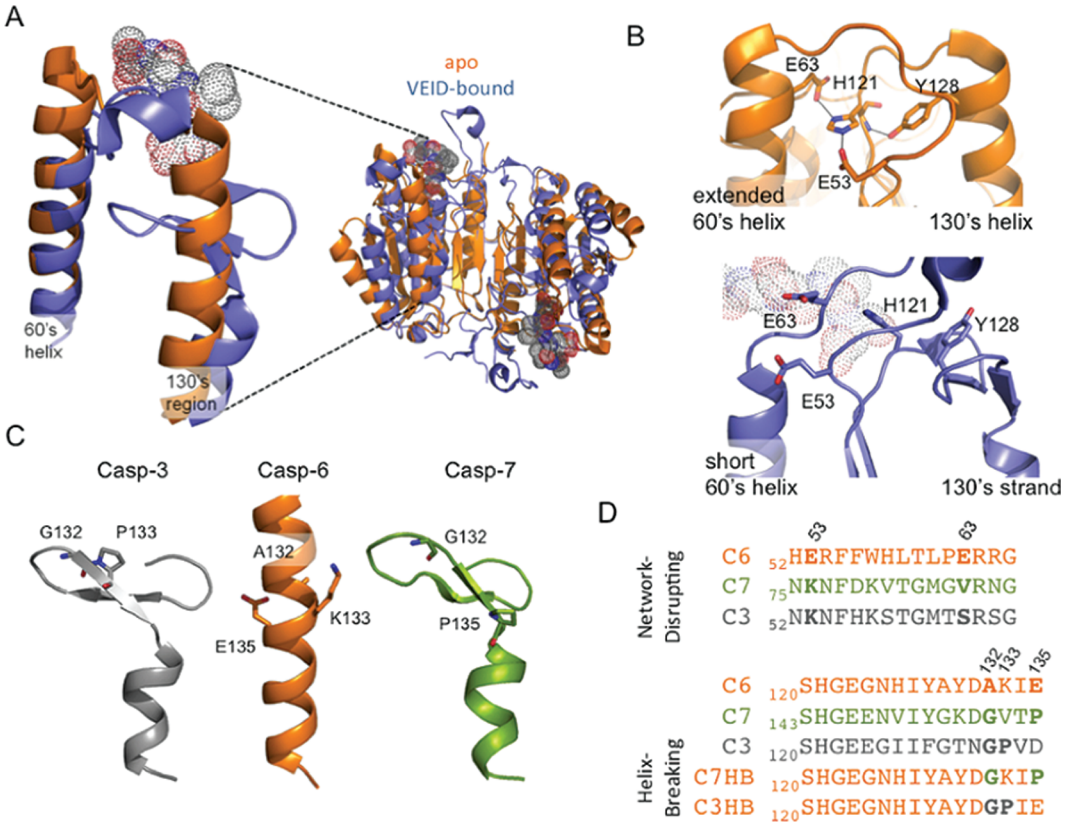

Figure 1. Caspase-6 latent state extended helices and helical network interrogated by mutations. (A) Overlay of apo mature caspase-6 (PDB entry 3NKF, orange) and active site-bound caspase-6 (PDB entry 3OD5, blue). Two extended helices, the 130's and 60's helices, are lost upon ligand binding. The ligand VEID (dots) bound in the substrate-binding groove is incompatible with the extended helical conformation. (B) The helix-bridging network (residues E63, H121, E53, and Y128), which is only present in apo mature caspase-6 (orange), is broken in caspase-6 (blue) bound to VEID (dots). (C) The 130's region in apo caspase-3, -6, and -7 is helical only in caspase-6. Helix-breaking residues at positions 132, 133, and 135 in caspase-3 and -7 and the corresponding residues in caspase-6 (sticks) are located in the segment that undergoes a conformational change. (D) Sequence alignment of the 60's and 130's region in caspase-3, -6, and -7 inspired the design of the network-disrupting and helix-breaking (C3HB and C7HB) variants.

glutamate only in caspase-6, underscoring the uniqueness of this bridging network. When substrate binds, the top of the 130's helix (containing Tyr128) transforms into a strand, the top of the 60's helix (containing Glu63) transforms into a loop, the L1 loop (containing Glu53) changes conformation, and the helix-bridging network is broken (Figure 1B).

Comparison of the 130's helix sequence in caspase-6 with that from other executioner caspases provides a second insight into why only caspase-6 can form the extended, helical conformation. Prolines and glycines are typically considered to be helix-breaking residues, although they have been observed in helices and their removal does not always lead to a change in the helical conformation.[10,11] The most closely related caspases, caspase-3 and -7, contain helix-breaking residues in the 130's region, whereas caspase-6 has none. Gly and Pro are seen in caspase-3 (residues 132 and 133, respectively) and in caspase-7 (residues 133 and 135, respectively), but there are no glycines and prolines in this region of caspase-6 (Figure 1C,D). Pairs of helix-breaking residues are also present in the 130's region of all other caspases, suggesting their importance in preventing the helical conformation. On the basis of sequence alone, it appears that the 130's region of caspase-6 has a stronger propensity to adopt a helical conformation than other caspases.

The central motive behind this work is to understand the contributions of the helix-bridging network (Figure 1B) and the helix-breaking residues in the 130's region (Figure 1C,D) in maintaining the helical conformation of mature caspase-6. Toward this end, we introduced helix network-disrupting residues to mimic the residues present in caspase-7 and prevent formation of the hydrogen-bond network (E53K, E63V, and E53K/E63V). We also introduced helix-breaking residues into the 130's helix to generate the caspase-7-like helix-breaking variant (C7HB, containing the A132G and E135P substitutions) and the caspase-3-like helix-breaking variant (C3HB, containing the A132G and K133P substitutions) (Figure 1D). All of the variants are active, as assessed by cleavage of fluorescent substrate, and have k_{cat} and K_M values similar to those of the wild-type protein (Table 1), suggesting that these unique sequences are not required for the catalytic properties of caspase-6.

We have previously shown that caspase-6 exhibits a unique signature in the circular dichroism (CD) spectra at 222 nm resulting from the loss of the 130's and 60's helices upon substrate binding (Figure 2).[7,9] We have observed that in caspase-3 and caspase-7, caspases for which there is no evidence of the extended helical conformation, there is a very small change or no change in the 222 nm CD signal upon active-site ligand binding (Figure 2). We use this CD signature to monitor the effect of the helical network-disrupting and helix-breaking substitutions on the structure of the 130's and 60's region. The spectra of each of the apo (unliganded) variants were first

dx.doi.org/10.1021/bi2001664 |*Biochemistry* 2011, 50, 3282–3287

Table 1. Kinetic Parameters and Melting Temperatures for Wild-Type (WT) Caspases, the Network Disrupters, and the Helix Breakers[a]

	K_M (μM)	k_{cat} (s^{-1})	apo T_m (°C)	active site-bound T_m (°C)	ΔT_m (°C)
WT casp-6[b]	66 ± 7	0.81 ± 0.01	77 ± 0.5	80.3 ± 0.4	3.3
WT casp-3	5[c]	9.1[c]	83	>90	>7
WT casp-7[d]	23 ± 2	0.35 ± 3 × 10^{-3}	59.8 ± 0	77.7 ± 3.8	17.9
E53K	100 ± 28	0.7 ± 0.07	77 ± 0.1	77.2 ± 0.4	0.2
E63V	121 ± 24	0.78 ± 0.08	74.6 ± 1.5	77.5 ± 0.1	2.9
E53K/E63V	68 ± 16	0.74 ± 0.06	75.5 ± 0.2	78.3 ± 0.8	2.8
C3HB (A132O/K133P)	46 ± 3.5	0.84 ± 0.06	70.7 ± 1.0	76.5 ± 0.7	5.8
C7HB (A132G/E135P)	79 ± 13	1.2 ± 0.03	73.1 ± 0.5	77.8 ± 0.3	4.7

[a] K_M, k_{cat}, and T_m were measured in triplicate from samples independently prepared on three separate days. [b] Reported in ref 9. [c] Reported in ref 17. [d] Reported in ref 18.

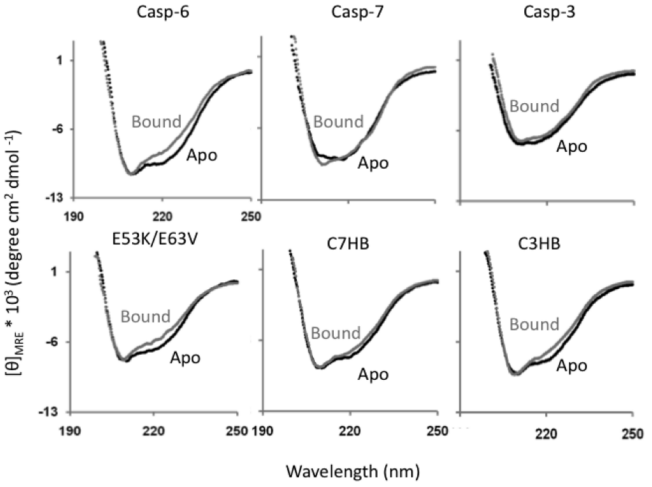

Figure 2. CD spectra of apo and ligand-bound wild-type caspase-6 reflect the change in structure of the 60's and 130's helix upon ligand binding. In contrast, the CD spectra of caspase-7 and -3 do not reflect a change in helical content. The network-disrupting variant (E53K/E63V) shows a similar change in helical content upon ligand binding to wild-type caspase-6. The helix-breaking variants C7HB and C3HB exhibit a much decreased difference in CD spectra between the apo and ligand-bound states, suggesting that the apo state is less helical in solution than wild-type caspase-6.

compared to that of wild-type caspase-6. Only C3HB exhibited a weaker CD signal at 222 nm (Figure S1 of the Supporting Information), indicating a decrease in helical content upon helix breaking relative to that of wild-type capase-6. An overlay of the CD spectra of apo and active-site ligand (VEID, a covalent aldehyde-based peptide inhibitor) bound caspase-6 reveals that the 130's helix-breaking mutants, C3HB and C7HB, have a smaller difference in the CD signal at 222 nm between apo and bound forms than wild-type caspase-6 (Figure 2). This smaller difference suggests that the apo state of C3HB and C7HB is more similar to the ligand-bound state (like caspase-3 and -7) than is the case for the wild type. Conversely, the network-disrupting variants exhibit a difference in the CD signal similar to that of wild-type caspase-6. This suggests that the network-disrupting variants are as helical as the wild type in the apo state. These data suggest that the absence of helix-breaking residues is more critical to the formation of the caspase-6 extended helices than the bridging hydrogen-bond network.

The melting temperature of a protein reflects the stability of that protein and the equilibria between folded and unfolded states. To assess the role of the helix network and the lack of helix-breaking residues in stability, the apo and VEID-bound forms of all the variants were also thermally denatured as monitored by CD. Among the variants, with the exception of E53K, all of the helix-breaking and network-disrupting variants have somewhat lower melting temperatures (T_m) than wild-type caspase-6 in both the apo and ligand-bound states (Table 1). The E53K and E63V mutations do not affect the T_m of the apo and bound forms significantly. However, the T_m of apo C3HB is 6.3 °C lower than that of apo wild-type caspase-6. The T_m of C7HB is 3.9 °C lower than that of apo wild-type caspase-6. Thus, introducing helix-breaking mutations into the 130's helix destabilizes the apo form and underscores the importance of the 130's helix in the stability of apo caspase-6.

The values of ΔT_m (apo vs ligand-bound) showed an increase in stability upon ligand binding for both caspase-7 (18 °C) and caspase-3 (>7 °C), with no significant conformational changes in the 130's region (Table 1). The increase in the T_m for caspase-3 may be as large as that of caspase-7 but cannot be measured because ligand-bound caspase-3 melts above 90 °C (the detection limit in water). In both caspase-3 and -7, no conformational changes in the 130's region are observed upon ligand binding, but a number of new interactions are formed. These interactions between the substrate binding loops and across the dimer interface can only occur when ligand binds and thereby orders the loops. These interactions contribute significantly to the high stability of the ligand-bound state of caspase-3 and -7. In contrast, the change in T_m is only 2−3 °C for WT caspase-6 upon substrate binding, denoting that the apo helical state and the strand-containing ligand-bound states of caspase-6 have similar stabilities, despite their large conformational differences. The C3HB and C7HB variants exhibit ΔT_m values of 5.8 and 4.7 °C, respectively, which are greater than the wild-type ΔT_m. A change in the magnitude of the ΔT_m for C3HB and C7HB suggests that these variants populate the extended helical conformation and ligand-bound (strand) conformation to different extents in the apo state compared to wild-type caspase-6. On the basis of the CD spectra and the T_m values, the sequence of the 130's helix, particularly the absence of helix-breaking residues, appears to be more critical for maintaining the helical conformation in apo caspase-6 than the helix-bridging network.

We used data from caspase-6 and caspase-7 to construct an energy diagram (Figure 3) with points representing the fully

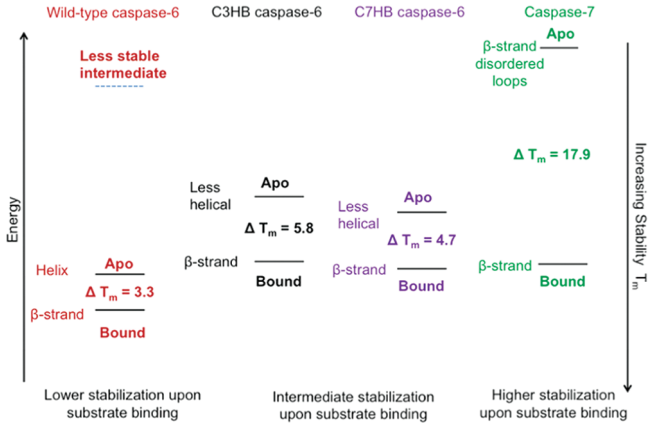

Figure 3. Relative stabilities of the apo and active site ligand-bound forms of caspase-6 and -7 and the helix-breaking C3HB and C7HB variants and the predicted caspase-6 intermediate.

β-strand conformation of the 130's region with disordered substrate-binding loops (apo caspase-7), the fully β-strand conformation of the 130's region with ordered substrate binding loops (bound caspase-6 or -7), and the fully helical conformation of the 130's region (apo caspase-6). Each of these states has a unique stability (T_m). Using these end points, we can then assess the contribution of each state to the conformation of the helix-breaking variants.

Caspase-6 undergoes a conformational change in the 130's helix to bind ligand but has a much smaller increase in stability upon ligand binding than other caspases. In addition, it is clear from crystal structures of caspase-6 that the extended conformation is incompatible with substrate binding. Thus, it appears that the change in conformation of the 130's helix causes apo-caspase-6 to undergo a transition through a less stable (high-energy) intermediate to attain the strand conformation that is compatible with binding ligand (Figure 3). This hypothesis is supported by the properties of the C3HB and C7HB variants, which, as assessed by CD, populate the helical conformation in the apo state to a lower degree than wild-type caspase-6. They also show greater stabilization (greater ΔT_m) upon ligand binding than wild-type caspase-6. This is because a larger fraction of the equilibrium apo population of these variants is in the strand conformation, like that seen in caspase-7. The high stability of the apo state of caspase-6 afforded by the extension of two helices may play a protective role, prolonging the lifetime of caspase-6.

The conformational switch in caspase-6 upon substrate binding is unique among proteases to caspase-6 but is not unprecedented in proteins generally. In the elongation factor, Ef-Tu, the effector C-terminus forms an α-helix when bound to GTP but converts to a β-hairpin upon GTP hydrolysis.[12] The evolution of Cro family proteins is another excellent paradigm for secondary structural α-to-β switches.[13] While the C-terminus of bacteriophage P22 Cro forms an α-helix, the homologous λ Cro forms a β-hairpin. α-to-β conformational switches are likewise critical for the propagation of prion infections.[14] Thus, structural switches regulate function and facilitate new biological roles.

Several new roles may be allowed by the helical conformation of the caspase-6 latent state. Both apoptotic and inflammatory caspases can perform functions independent of their catalytic activity. Caspase-1 and -2 can noncatalytically activate NF-κB; caspase-8 can be activated by c-FLIP$_L$, a catalytically inactive caspase, and functional caspase-12 exists in two catalytically inactive forms (for a review, see ref 15). We suspect that caspase-6 in the latent conformation may likewise perform noncatalytic functions. The absence of helix-breaking residues and the stable latent state may explain the resistance of caspase-6 to binding inhibitors in the active site. Intriguingly, the inhibitors of apoptosis (IAPs) bind and inhibit the active sites of caspase-3 and -7 but not of caspase-6.[16] The conformation of IAPs bound to caspases appears to be structurally incompatible with the latent state of caspase-6 (Figure S2 of the Supporting Information). Thus, it is likely that formation of the latent state prevents IAP binding. The lack of IAP binding potentially improves the response of caspase-6 to substrate or to other noncatalytic stimuli.

In conclusion, our two major findings address why caspase-6 can uniquely adopt the helical latent state. First, upon substrate binding, part of the extended 130's helical region switches to a β-strand conformation through a high-energy, substrate-compatible intermediate. Second, the absence of helix-breaking residues is critical to the extended conformation of the 130's helix region in the latent state structure of caspase-6, whereas the hydrogen-bond network in this region is not essential. Given the important role caspase-6 plays in a number of neurodegenerative diseases, these two findings may be exploited in the design of small molecule inhibitors that are specific for caspase-6, either binding to the extended helical (latent) state or preventing the transition through the high-energy intermediate required for substrate binding.

MATERIALS AND METHODS

Generation of Caspase-6 Variants. A synthetic *Escherichia coli* codon-optimized His-tagged casp-6 gene coding for amino acids 24−293 (ΔN D179A) in pET11a vector (Stratagene) produced for earlier studies[9] was used for generating the variants. The mutations E53K, E63V were introduced in the caspase-6 ΔN D179A gene construct by Quikchange site-directed mutagenesis method (Stratgene). The E63V mutation was introduced into E53K ΔN D179A construct to make the E53K/E63V double mutant. The A132G/E135P (C7HB) and A132G/K133P (C3HB) variants were generated by simultaneously introducing A132G, E135P and A132G, K133P mutations into the ΔN D179A construct.

Expression and Purification . The caspase-6 variants in pET11a vectors were transformed into the BL21(DE3) T7 express strain of *E. coli* (NEB). The cultures were grown in 2×YT media with Amp (100 mg/L, Sigma-Aldrich) at 37 °C until they reached OD_{600} = 0.6. The temperature was reduced to 20 °C and cells were induced with 1 mM IPTG (Anatrace) to express soluble His-tagged protein. Cells were harvested after 18 h for all other variants to ensure complete processing. Cell pellets stored at −20 °C were freeze-thawed and lysed in a microfluidizer (Microfluidics, Inc.) in 300 mM NaCl, 2 mM imidazole, 5% glycerol, 50 mM Tris pH 8.6. Lysed cells were centrifuged at 17 K rpm to remove cellular debris. The filtered supernatant was loaded onto a 5 mL HiTrap Ni-affinity column (GE Healthcare). The column was washed with 300 mM NaCl, 50 mM imidazole, 5% glycerol, 50 mM Tris pH 8.6, and the protein was eluted with 300 mM NaCl, 250 mM imidazole, 5% glycerol, 50 mM Tris pH 8.6. The eluted fraction was diluted by 5-fold into 2 mM DTT, 20 mM Tris pH 8.6 buffer to reduce the salt concentration. This protein sample was loaded onto a 5 mL Macro-Prep High Q

column (Bio-Rad Laboratories, Inc.). The column was developed with a linear NaCl gradient and eluted in 120 mM NaCl, 2 mM DTT, and 20 mM Tris pH 8.6 buffer. The eluted protein was stored at −80 °C in the above buffer conditions. The purity of the caspase-6 variants was analyzed by SDS−PAGE.

Activity Assays. For kinetic measurements of caspase activity, 100 nM freshly purified protein (within hours of purification and without ever being frozen, to prevent changes in cleavage pattern or activity) was assayed over the course of 7 min in a caspase-6 activity buffer containing 100 mM HEPES pH 7.5, 10% sucrose, 0.1% CHAPS, 5 mM DTT, and 30 mM NaCl.[19] For substrate titrations, a range of 0−500 μM fluorogenic substrate, VEID-AMC, (*N*-acetyl-Val-Glu-Ile-Asp- (7-amino-4-methylcoumarin), Enzo Lifesciences) Ex365/Em495, was added to initiate the reaction. Assays were performed in duplicates at 37 °C in 100 μL volumes in 96-well microplate format using a Molecular Devices Spectramax M5 spectrophotometer. Initial velocities versus substrate concentration were fit to a rectangular hyperbola using GraphPad Prism (Graphpad Software) to determine kinetic parameters K_m and k_{cat}. For some of the mutants we observed an approximately 2-fold change in K_m. This modest change in K_m may be due to the contribution of the change in the equilibrium of the strand versus helical states. Enzyme concentrations were determined by active site titration with quantitative, inhibitor VEID-CHO (*N*-acetyl-Val-Glu-Ile-Asp-Aldehyde, Enzo Lifesciences). Active site titrations were incubated over a period of 2 h in 120 mM NaCl, 2mM DTT, 20 mM Tris pH 8.5 at nanomolar concentrations. Optimal labeling was observed when protein was added to VEID-CHO solvated in dimethylsulfoxide in 96-well V-bottom plates, sealed with tape, and incubated at room temperature in a final volume of 200 μL. 90 μL aliquots were transferred to black-well plates in duplicate and assayed with a 50-fold molar excess of substrate. The protein concentration was determined to be the lowest concentration at which full inhibition was observed.

Secondary Structure Prediction . Sequences of wild-type and variants ranging from residues 120−141 which include the 130's region and the loop above 130's region were analyzed for secondary structure using the expasy server using the Hierarchical Neural Network method (http://npsa-pbil.ibcp.fr/cgibin/ npsa_automat.pl?page=npsa_nn.html).

Secondary Structure and Stability Measurements by Circular Dichroism. Active-site liganded caspase-6 variants were prepared by 2-h room temperature incubation with 3 molar equivalents of VEID-CHO (*N*-acetyl-Val-Glu-Ile-Asp-aldehyde, Enzo Lifesciences) at a concentration of 6−12 μM in 120 mM NaCl, 2 mM DTT, 20 mM Tris, pH 8.6 3 buffer. Caspase-7, -3 samples were prepared in a similar fashion by incubating with DEVD-CHO (*N*-acetyl-Asp-Glu-Val-Asp-aldehyde, Enzo Lifesciences). To ensure complete binding of active-site ligand to the protein, the protein was assayed with a 50 molar excess of substrate VEIDAMC for caspase-6 and DEVD-AMC (*N*-acetyl-Asp-Glu-Val-Asp-AMC (7-amino-4-methylcoumarin)) for caspase-7, -3. A 95−97% inhibition was observed indicating that the protein was fully occupied with the substrate mimic. Liganded and apo proteins were then buffer exchanged six times (7-fold dilution each time) into 10 mM phosphate buffer, pH 7.5 with 120 mM NaCl using Vivaspin 500, 3 K MWCO membrane concentrators (Sartorium Stedim Biotech) for repeated dilution and buffer exchange. After buffer exchange, the final concentration of DTT was ∼10 nM. A protein concentration of ∼6 μM for caspase-6, -7 and ∼4 μM for caspase-3 as assessed by absorbance at 280 nm (Nanodrop 2000C spectrophotometer) were used for analysis. A similar procedure was followed to prepare sample for apo protein without the active-site ligand.

Thermal denaturation of caspase-6 variants was monitored by loss of circular dichroism signal at 222 nm over a range of 12−90 °C and CD spectra (250−190 nm) were measured on a J- 720 circular dichroism spectrometer (Jasco) with a peltier controller. The temperature was increased at a rate of 1° per min. We found that this rate of temperature increase is appropriate for this analysis as we have found that 1 min is sufficient to fully unfold caspase-6 in 8 M urea (data not shown). The CD spectra ranging from 190 to 270 nm were collected for the apo and ligand-bound forms before and after thermal denaturation. All data were collected in duplicates on separate days. The thermal denaturation data was fit using Origin Software (OriginLab) using sigmoid fit to determine the melting temperature.

■ ASSOCIATED CONTENT

Supporting Information. Supporting Figures S1 and S2. This material is available free of charge via the Internet at http://pubs.acs.org.

■ AUTHOR INFORMATION

Corresponding Author

*Phone: (413) 545-3486. Fax: (413) 545-4990. E-mail: hardy@chem.umass.edu.

Funding Sources

This work was supported by National Institutes of Health Grant R01 GM080532.

■ ACKNOWLEDGMENT

We thank Elih Velázquez for caspase-3 purification and T_m and Witold Witkowski for purified caspase-7.

■ REFERENCES

(1) Nikolaev, A., McLaughlin, T., O'Leary, D., and Tessier-Lavigne, M. (2009) APP binds DR6 to trigger axon pruning and neuron death via distinct caspases. *Nature 457*, 981–989.

(2) Watanabe, C., Shu, G., Zheng, T., Flavell, R., and Clark, E. (2008) Caspase 6 regulates B cell activation and differentiation into plasma cells. *J. Immunol. 181*, 6810–6809.

(3) Klaiman, G., Petzke, T., Hammond, J., and LeBlanc, A. (2008) Targets of caspase-6 activity in human neurons and Alzheimer disease. *Mol. Cell. Proteomics 7*, 1541–1555.

(4) Galvan, V., Gorostiza, O., Banwait, S., Ataie, M., and Logvinova, A. (2006) et al. Reversal of Alzheimer's-like pathology and behavior in human APP transgenic mice by mutation of Asp664. *Proc. Natl. Acad. Sci. U.S.A. 103*, 7130–7135.

(5) Graham, R., Deng, Y., Slow, E., Haigh, B., and Bissada, N. (2006) et al. Cleavage at the caspase-6 site is required for neuronal dysfunction and degeneration due to mutant huntingtin. *Cell 125*, 1179–1191.

(6) Giaime, E., Sunyach, C., Druon, C., Scarzello, S., and Robert (2009) et al. Loss of function of DJ-1 triggered by Parkinson's disease-associated mutation is due to proteolytic resistance to caspase-6. *Cell Death Differ. 17*, 158–169.

(7) Wang, X. J., Cao, Q., Liu, X., Wang, K. T., and Mi, W. (2010) et al. Crystal structures of human caspase 6 reveal a new mechanism for intramolecular cleavage self-activation. *EMBO Rep. 11*, 841–847.

(8) Baumgartner, R., Meder, G., Briand, C., Decock, A., and D'Arcy, A. (2009) et al. The crystal structure of caspase-6, a selective effector of axonal degeneration. *Biochem. J. 423*, 429–439.

(9) Vaidya, S., Velazquez-Delgado, E. M., Abbruzzese, G., and Hardy, J. A. (2011) Substrate-induced conformational changes occur in all cleaved forms of caspase-6. *J. Mol. Biol. 406*, 75–91.

(10) Alber, T., Bell, J. A., Sun, D. P., Nicholson, H., Wozniak, J. A., Cook, S., and Matthews, B. W. (1988) Replacements of Pro86 in phage T4 lysozyme extend an alpha-helix but do not alter protein stability. *Science 239*, 631–635.

(11) Hardy, J. A., and Nelson, H. C. (2000) Proline in alpha-helical kink is required for folding kinetics but not for kinked structure, function, or stability of heat shock transcription factor. *Protein Sci. 9*, 2128–2141.

(12) Polekhina, G., Thirup, S., Kjeldgaard, M., Nissen, P., Lippmann, C., and Nyborg, J. (1996) Helix unwinding in the effector region of elongation factor EF-Tu-GDP. *Structure 4*, 1141–1151.

(13) Newlove, T., Konieczka, J., and Cordes, M. (2004) Secondary structure switching in Cro protein evolution. *Structure 12*, 569–581.

(14) Pan, K., Baldwin, M., Nguyen, J., Gasset, M., and Serban, A. (1993) et al. Secondary structure switching in Cro protein evolution. *Proc. Natl. Acad. Sci. U.S.A. 90*, 10962–10966.

(15) Lamkanfi, M., Festjens, N., Declercq, W., Vanden Berghe, T., and Vandenabeele, P. (2007) Caspases in cell survival, proliferation and differentiation. *Cell Death Differ. 14*, 44–55.

(16) Deveraux, Q., Takahashi, R., Salvesen, G., and Reed, J. (1997) X-linked IAP is a direct inhibitor of cell-death proteases. *Nature 388*, 300–304.

(17) Thornberry, N. A., Rano, T. A., Peterson, E. P., and Rasper, D. M. (1997) et al. A combinatorial approach defines specificities of members of the caspase family and granzyme B. Functional relationships established for key mediators of apoptosis. *J. Biol. Chem. 272*, 17907–17911.

(18) Witkowski, W. A., and Hardy, J. A. (2009) L2' loop is critical for caspase-7 active site formation. *Protein Sci. 18*, 1459–1468.

(19) Stennicke, H. R., and Salvesen, G. S. (1997) Biochemical characteristics of caspases-3, -6, -7, and -8. *J. Biol. Chem. 272*, 25719–25723.

■ NOTE ADDED AFTER ASAP PUBLICATION

This paper was published on the Web on March 17, 2011. The Materials and Methods section was added to the text, and the corrected version was reposted on March 31, 2011.